

Foam Ratio as a Measure for Mechanical Foam-Breaking in Gas Bubbling Systems

Masami YASUKAWA, Kazuaki YAMAGIWA, and Akira OHKAWA*

Department of Material and Chemical Engineering, Faculty of Engineering,
The University of Niigata, Ikarashi, Niigata 950-21

(Received February 9, 1990)

The volume fraction of liquid in foam, designated as the foam ratio, was measured for a gas-bubbling system using various foaming liquids. The foam ratio can be used as a substantial measure of the dynamic foaming capacity for gas-bubbling systems. The applicability of the foam ratio for evaluating the performance of mechanical foam-breaking was investigated. Furthermore, the effect of the operating conditions on the foam ratio was related to the extent of mechanical foam-breaking.

Foaming is a rather common phenomenon in chemical industries. It appears extensively not only in microbial processes, such as fermentation and wastewater treatment, but also in factories such as textiles, paper pulping, food manufacturing. Though foaming causes various problems in production processes,¹⁾ it has a beneficial utilization in techniques of foam separation and ore flotation.²⁾ Antifoam agents have been employed in many places to control foaming. However, the addition of antifoam agents to a process solution involves the following problems:^{3–5)} (1) a reduction of the oxygen-transfer rate; (2) reaction inhibition and toxicity; (3) adverse effects on the separation and purification of products. In view of these facts, foam-breaking by a mechanical force is desirable. Though a number of mechanical foam-breaking methods have so far been proposed, most of these techniques are hardly practical for foam-breaking operation in high-rate gas bubbling systems of industrial scale.^{3–5)} There are various methods proposed for measuring the nature of foam such as surface viscosity, surface elasticity, and surface rigidity.^{6–9)} Most of these methods, however, could allow measurements under considerably restricted conditions that are different from actual gas bubbling and foaming. Therefore, a direct application of these methods to a mechanical foam-breaking system under high gas throughput is difficult. In order to improve the existing foam-breaking system, or to develop a foam-breaker having high performance, it is important for it to be based on a measure that reflects the dynamic foaming capacity in a gas-bubbling system. However, little information is available on such a measure. Previously, we examined the rotating-disk foam-breaker (MFRD) as a foam-breaking apparatus.^{10,11)} In a gas-bubbling system using a dilute detergent solution, we also showed that the foam ratio, viz., the volume fraction of liquid in the foam, affected the foam-breaking capacity of MFRD.¹²⁾

In this study, the foam ratio was first measured for a gas-bubbling system using various foaming liquids under mechanical foam-breaking with MFRD. The effect of the operating conditions on the foam ratio

was observed. Here, the relation between the foam ratio and the power for foam-breaking is also discussed. The applicability of the foam ratio to different foam-breaking system is also examined.

Experimental

Apparatus. The experimental set-up is shown in Fig. 1. For a gas-liquid contactor used as a gas-bubbling system, a vessel of 0.23 m in diameter, D_T , which was equipped with six ball spargers in diameter with average pore openings of 25 μm and four baffle plates (0.1 D_T in width), was used. The liquid volume, V , in the vessel and the gas velocity, U_g , on the cross-sectional area of the vessel were varied over the range 4.0×10^{-3} to $7.0 \times 10^{-3} \text{ m}^3$ and 1.41×10^{-3} to $5.62 \times 10^{-3} \text{ m s}^{-1}$, respectively. A MFRD (rotating disk of 0.18 m in diameter D_d) was set in the head space of the vessel, holding the ratio of D_T to the disk height, H_d , at 0.85. The liquid feed rate, W , onto the rotating disk was kept at 1.0×10^{-5}

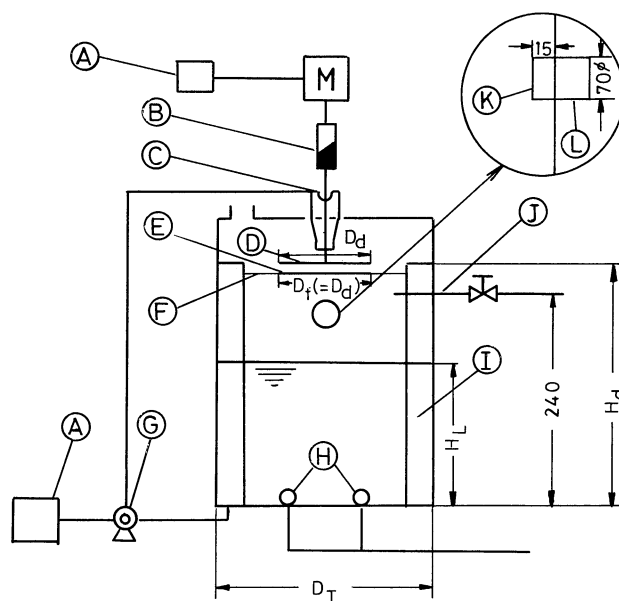


Fig. 1. Experimental apparatus (unit: mm). A, controller; B, torque meter; C, liquid feeder; D, rotating disk; E, fixed disk; F, supporting bar of fixed disk; G, roller pump; H, ball sparger; I, baffle plate; J, foam sampling tube; K, window; L, column.

$\text{m}^3 \text{s}^{-1}$. Further details regarding the apparatus and experimental methods were given in the previous papers.^{11,12)}

Both the spray nozzle (SN)¹³⁾ and the fluid-impact dispersion apparatus (FIDA)¹⁴⁾ shown in Fig. 2 were used as foam-breakers in the same foam-breaking mechanism as of MFRD.

In this equipment, liquid particles formed by spewing the pressure-driven liquid are dispersed radially. SN or FIDA was set as the same height as in the case of MFRD. The liquid feed rate, W_c , through SN and FIDA ranged from 3.29×10^{-5} to $6.08 \times 10^{-5} \text{ m}^3 \text{s}^{-1}$ and from 2.96×10^{-5} to $5.00 \times 10^{-5} \text{ m}^3 \text{s}^{-1}$, respectively. Full details regarding SN and FIDA are available elsewhere.¹¹⁾

Foam Ratio. Foam withdrawn through a length-variable glass tube fitted on the wall was collected in a graduated container of constant volume, V_F .¹²⁾ The local foam ratio, ϕ_L , at different radial positions from the vessel wall was determined by

$$\phi_L = \frac{V_L}{V_F}, \quad (1)$$

where V_F is the foam volume and V_L is the net liquid volume in V_F . The value of V_L was measured from spontaneous collapse of foam in the container.

Foam Size. Photographs of ascending foams were taken through a column window (0.07 m in diameter), as shown in Fig. 1. The bubble shape could be approximated as being a sphere, and the arithmetic mean diameter, d_B , was then calculated for bubbles of more than 100 pieces.

Foaming Liquid. Fifty eight kinds of foaming liquids were used. The kinds of the liquids are summarized in Table 1 together with the physical properties of the liquids.

Results and Discussion

Local Foam Ratio. The local foam ratio, ϕ_L , was determined at a transient state, which is in the regime of foam-breaking to non-foam-breaking as a critical foam-breaking state.^{10–12)}

Figure 3a and 3b show the typical distribution of ϕ_L with varying the gas velocity, U_g , and the liquid volume, V , in the vessel. In the figures, ϕ_L is plotted against the radial distance, R , from the wall. Although there is a difference in the value of ϕ_L , depending on the liquids, all the systems used had a tendency that ϕ_L became larger when U_g and V was increased. In addition, the value of ϕ_L was large at a position close to the vessel wall. The main cause was due to the situation that the collapsed foam liquid produced by foam-breaking tended to flow downward along with the wall.

Effect of Operating Conditions on Averaged Foam Ratio. Mechanical foam-breaking by MFRD utilizes the impact of liquid particles dispersed from the

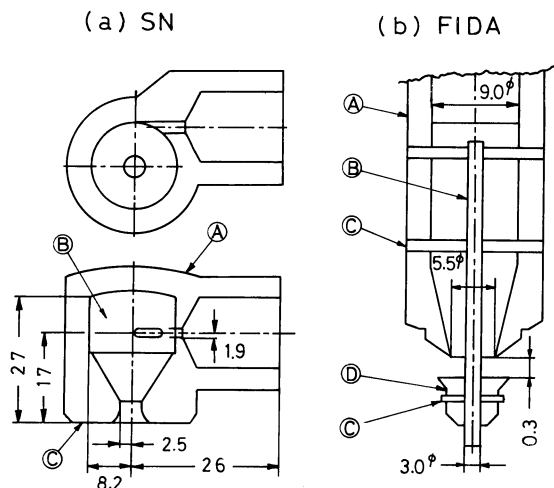


Fig. 2. (a) Structure and dimension (in mm) of SN; (A) body, (B) chamber, and (C) head. (b) Structure and dimension (in mm) of FIDA; (A) nozzle, (B) fixed axis, (C) set screw, and (D) impact plate.

Table 1. Physical Properties of Foaming Liquids at 293 K

Solution	Concentration/%	$\rho/\text{kg m}^{-3}$	$\mu/\text{mPa s}$	$\sigma/\text{mN m}^{-1}$
Detergent ^{c)}	$3.0 \times 10^{-3} - 1.0 \times 10^{-2a)}$	998.2	1.00	53.94–70.00
Tween 40	$5.0 \times 10^{-3} - 5.0 \times 10^{-2b)}$	998.4	1.02	50.30–61.45
Tween 60	$5.0 \times 10^{-2} - 1.0 \times 10^{-1b)}$	998.4	1.02	45.20–51.50
Albumin	$5.0 \times 10^{-1} - 1.0^b)$	999.4–1000.4	1.06–1.07	48.90–51.60
Soybean meal ^{d)}	$0.50 - 3.0^b)$	998.9–1001.5	1.05–1.19	48.19–57.31
Saponin	$1.0 \times 10^{-2b)}$	998.1	1.00	63.90
BSA ^{e)}	$1.0 \times 10^{-2b)}$	998.3–998.7	1.02	57.63–57.96
Baker's yeast ^{f)} +Detergent	$1.0 \times 10^{-2b)}$ in 0.1 mol% NaCl			
	$5.0 \times 10^{-1b)}$ + $4.8 \times 10^{-3a)}$	999.0–1007.0	1.02–1.22	49.70
	$1.0^b)$ + $6.3 \times 10^{-3a)}$			
Corn syrup+Detergent	$10 - 60^b)$ + $2.5 \times 10^{-2a)}$	1035.8–1235.5	1.25–9.77	46.48–58.55
Corn syrup+Tween 40	$10 - 60^b)$ + $5.0 \times 10^{-2b)}$	1035.8–1235.8	1.25–9.77	51.92–55.10
Corn syrup+Soybean meal	$10 - 60^b)$ + $3.0^b)$	1037.3–1236.8	1.39–9.91	52.52–56.08
Corn syrup+Saponin	$10 - 60^b)$ + $1.0 \times 10^{-2b)}$	1029.9–1334.8	1.26–8.26	63.71–70.64

a) Vol%. b) Wt%. c) Lipon F, manufactured by Lion Corp. (Non-ionic surfactant 23%, Sodium alkylbenzenesulfonate, Sodium alkylethersulfuricester). d) Liquid filtered after 1 h boiling. e) Bovine serum albumin. f) Wet yeast.

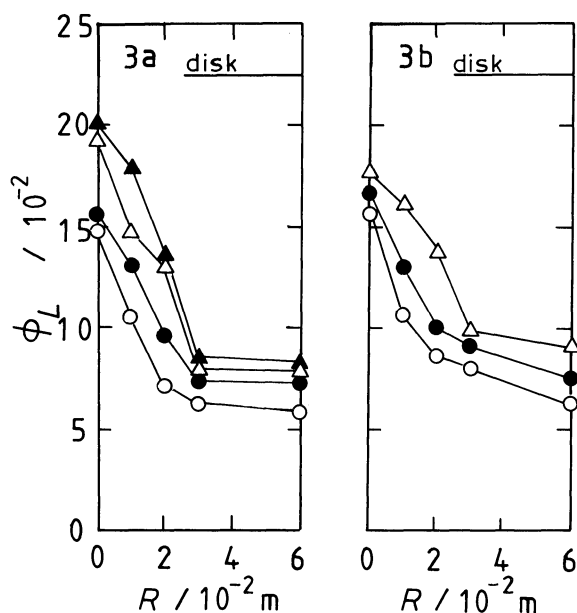


Fig. 3. Radial distribution of ϕ_L . 3a: (1.0×10^{-2} vol%) Detergent solution; $V = 7.0 \times 10^{-3} \text{ m}^3$; U_g (m s^{-1}): \circ ; 1.41×10^{-3} , \bullet ; 2.82×10^{-3} , Δ ; 4.21×10^{-3} , \blacktriangle ; 5.62×10^{-3} . 3b: (35 wt%) Corn-syrup + (1.0×10^{-2} wt%) Saponin solution; $U_g = 4.21 \times 10^{-3} \text{ m s}^{-1}$; V (m^3): \circ ; 4.0×10^{-3} , \bullet ; 5.5×10^{-3} , Δ ; 7.0×10^{-3} .

margin of a disk against the foam passing through an annular section between the disk and the vessel wall.¹²⁾ According to this mechanism, the mean value of ϕ_L on the annular section (that is, the averaged foam ratio $\bar{\phi}_L$) becomes important. Using ϕ_L data in Fig. 3 we evaluated $\bar{\phi}_L$ by means of graphical integration from the wall to the edge of the disk. Moreover, for constant values of D_T and H_d , the increase in the liquid volume V resulted in a decrease of the foam-ascending distance, h_f , from the aerated liquid surface. The value of h_f may be related to that of distance H_f between the disk height, H_d , and the static liquid height, H_L : $H_d - H_L$. We thus examined the variation of $\bar{\phi}_L$ with H_f and the gas velocity, U_g . Figure 4a shows a plot of $\bar{\phi}_L$ vs. U_g with H_f used as a parameter. It was found that $\bar{\phi}_L$ becomes larger as U_g increases and H_f decreases. This may be attributed to the increase in the liquid entrainment in the foam¹⁵⁾ and to a lowering of foam drainage by gravity as a result of the decrease in the ascending distance.¹⁶⁾

In MFRD, the degree of splashing of liquid particles from the disk depends on the rotation speed of the disk. Thus, the relation between the critical disk speed, N_c , required for foam-breaking and the value of $\bar{\phi}_L$ was examined. The results of N_c at the same operating conditions as in Fig. 4a are shown in Fig. 4b (the oblique-lined areas below respectively solid lines represent the region of non-foam breaking¹²⁾). N_c tends to raise with increasing U_g and with decreasing H_f . It was also found that the tendency of increasing

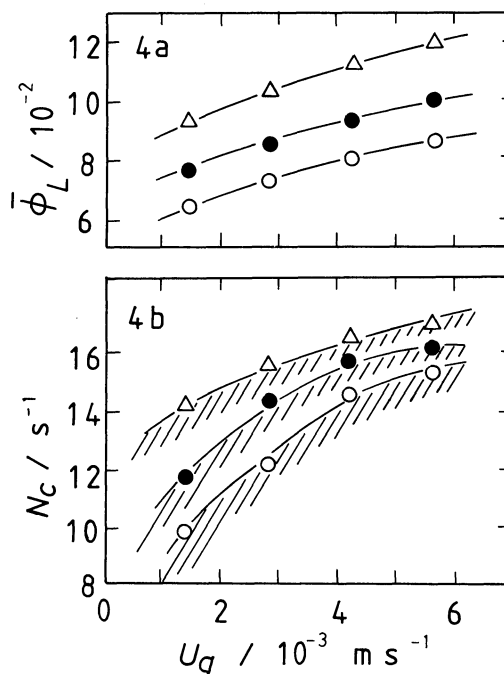


Fig. 4. Relation between U_g and $\bar{\phi}_L$ or N_c for a (35 wt%) Corn-syrup + (5.0×10^{-2} wt%) Tween 40 solution. 4a: $\bar{\phi}_L$ vs. U_g ; H_f (m): \circ ; 0.103, \bullet ; 0.140, Δ ; 0.176 4b: N_c vs. U_g (Keys are the same as in Fig. 4a).

N_c in Fig. 4b is similar to that of increasing $\bar{\phi}_L$ in Fig. 4a. According to this result, it should be noted that the value of N_c depends on $\bar{\phi}_L$.

Effect of Physical Properties on Averaged Foam Ratio. Figure 5 shows a plot of $\bar{\phi}_L$ against the surface tension, σ , of foaming liquids. It was difficult to observe the surface tension dependency of $\bar{\phi}_L$. One is liable to consider that the lowering of σ is one of the important conditions for forming foam. However, the lowering of σ is not necessarily related to the foaming ability. The results shown in Fig. 5 seem to support no surface tension dependency of the foaming ability.^{17,18)}

The relation between $\bar{\phi}_L$ and the kinematic viscosity, ν , is shown in Fig. 6. $\bar{\phi}_L$ tends to gradually decrease with increasing ν . In studies on foam separation using a foaming column,^{19,20)} it has been shown that an increase in the foam size, d_B , contributes to a decrease in the foam ratio. If this relation between d_B and the foam ratio applies to a mechanical foam-breaking system, it may be observed that d_B increases with increasing ν . Figure 7 shows a plot of d_B vs. ν . As was expected, d_B tends to increase with increasing ν . This result shows that the dependency of ν on $\bar{\phi}_L$ in Fig. 6 can be explained from the increase of d_B with increasing ν .

Relation between Averaged Foam Ratio and Foaminess. Although various measures to reflect the dynamic foaming capacity of a liquid are available,^{2,6,21,22)} the most typical measure is the foaminess,

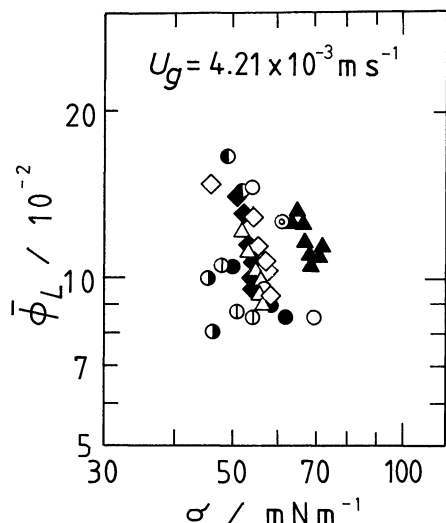


Fig. 5. Relation between $\bar{\phi}_L$ and σ at $V=7.0 \times 10^{-3} \text{ m}^3$. Foaming liquids: \circ ; (3.0×10^{-3} – 1.0×10^{-2} vol%) Detergent solutions, \bullet ; (5.0×10^{-3} – 5.0×10^{-2} wt%) Tween 40 solutions, \odot ; (5.0×10^{-2} – 1.0×10^{-1} wt%) Tween 60 solutions, \ominus ; (5.0×10^{-1} – 1.0 wt%) Albumin solutions, \oplus ; (0.50–3.0 wt%) Soybean meals, \otimes ; (1.0×10^{-2} wt%) Saponin solution, \diamond ; (10–60 wt%) Corn-syrup+(2.5×10^{-2} vol%) Detergent solutions, \blacklozenge ; (10–60 wt%) Corn-syrup+(5.0×10^{-2} wt%) Tween 40 solutions, \triangle ; (10–60 wt%) Corn-syrup+(3.0 wt%) Soybean meals, \blacktriangle ; (10–60 wt%) Corn-syrup+(1.0×10^{-2} wt%) Saponin solutions.

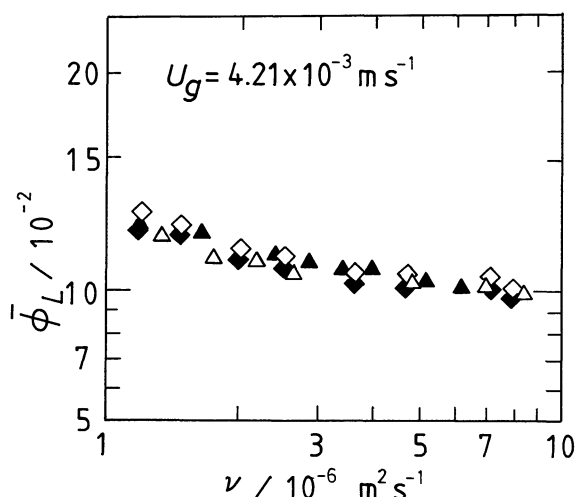


Fig. 6. Relation between $\bar{\phi}_L$ and ν at $V=7.0 \times 10^{-3} \text{ m}^3$ (Keys are the same as in Fig. 5).

Σ . If this Σ can be applied as a measure of mechanical foam-breaking to a gas-bubbling system, a proportional relation may be found between the values of $\bar{\phi}_L$ and Σ . The foaminess, Σ ,¹⁷⁾ is given by

$$\Sigma = \frac{V_s}{V_{tg}}, \quad (2)$$

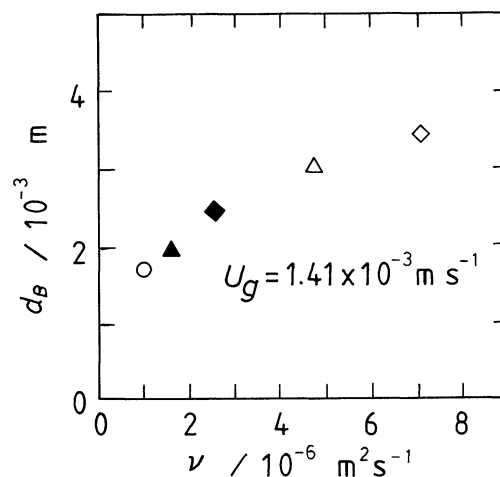


Fig. 7. Relation between d_B and ν at $V=7.0 \times 10^{-3} \text{ m}^3$. Foaming liquids: \circ ; (1.0×10^{-2} vol%) Detergent solution, \blacktriangle ; (20 wt%) Corn-syrup+(1.0×10^{-2} wt%) Saponin solution, \blacklozenge ; (35 wt%) Corn-syrup+(5.0×10^{-2} wt%) Tween 40 solution, \triangle ; (50 wt%) Corn-syrup+(3.0 wt%) Soybean meal, \diamond ; (60 wt%) Corn-syrup+(2.5×10^{-2} vol%) Detergent solution.

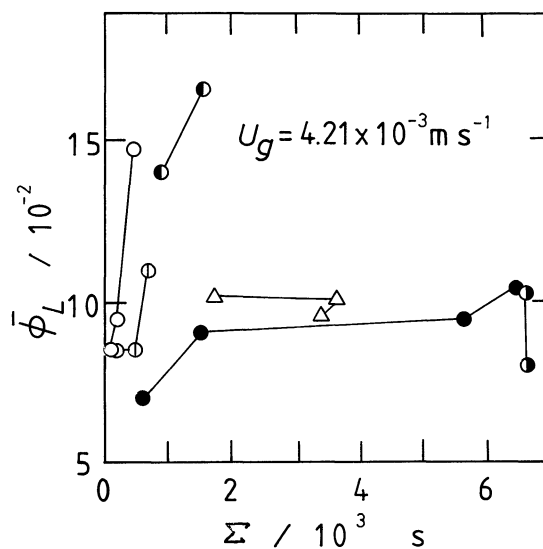


Fig. 8. Relation between $\bar{\phi}_L$ and Σ at $V=7.0 \times 10^{-3} \text{ m}^3$ (Keys are the same as in Fig. 5).

where V_s is the equilibrium volume of foam above the liquid layer and V_{tg} is the volumetric gas-flow rate. The Σ values for liquids were measured according to identical methods to those used by Kalischewski et al.²¹⁾

Figure 8 shows the results of $\bar{\phi}_L$ vs. Σ . It seems that there is no definite relation between the increases of $\bar{\phi}_L$ and Σ . In the measurement system of Σ , the equilibrium foam height in the vessel related to V_s depends on the liquid. This means that there is no restriction in the foam height in such a system. On the other hand, in a mechanical foam-breaking system where a foam-breaker is set in the foam-ascending sec-

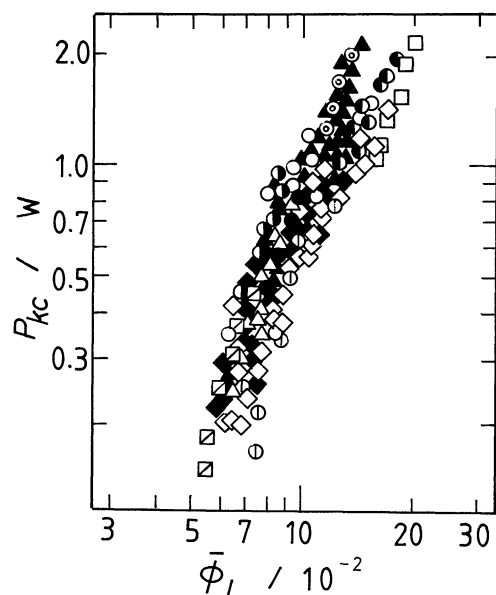


Fig. 9. Relation between $\bar{\phi}_L$ and P_{kc} . Forming liquids: \circ ; (3.0×10^{-3} — 1.0×10^{-2} vol%) Detergent solutions, \bullet ; (5.0×10^{-3} — 5.0×10^{-2} wt%) Tween 40 solutions, \odot ; (5.0×10^{-2} — 1.0×10^{-1} wt%) Tween 60 solutions, \ominus ; (5.0×10^{-1} — 1.0 wt%) Albumin solutions, Φ ; (0.50 — 3.0 wt%) Soybean meals, \otimes ; (1.0×10^{-2} wt%) Saponin solution, \square ; (1.0×10^{-2} wt%) BSA in water or in (0.1 mol%) NaCl solution, \boxplus ; (0.50 — 1.0 wt%) Yeast+ (4.8×10^{-2} — 6.3×10^{-2} vol%) Detergent solutions, \diamond ; (10 — 60 wt%) Corn-syrup+ (2.5×10^{-2} vol%) Detergent solutions, \blacklozenge ; (10 — 60 wt%) Corn-syrup+ (5.0×10^{-2} wt%) Tween 40 solutions, Δ ; (10 — 60 wt%) Corn-syrup+ (3.0 wt%) Soybean meals, \blacktriangle ; (10 — 60 wt%) Corn-syrup+ (1.0×10^{-2} wt%) Saponin solutions.

tion, there is obviously a restriction in the foam height. The main cause for the results in Fig. 8 seems to be due to these differences between the two measurement systems.

Relation between Averaged Foam Ratio and Power for Foam-Breaking. The power for foam-breaking with MFRD (power P_{kc} required for liquid dispersion by the rotating disk) was determined by

$$P_{kc} = 2\pi N_c \tau, \quad (3)$$

where τ is the net torque observed when the disk is rotated at the speed N_c . Figure 9 shows the relation between P_{kc} and $\bar{\phi}_L$ for all of the data. On the whole, the increase of P_{kc} and $\bar{\phi}_L$ correspond well. According to this result, it may be pointed out that the value of $\bar{\phi}_L$ can also be related to the extent of mechanical foam-breaking. Further information concerning the foam-ascending velocity and the bubble residence time in the foam layer will be necessary for a more detailed discussion on the relation between P_{kc} and $\bar{\phi}_L$.

Applicability of Foam Ratio to Mechanical Foam-Controlling Systems with Other Configurations of Foam-Breakers. The averaged foam ratio, $\bar{\phi}_L$, on the

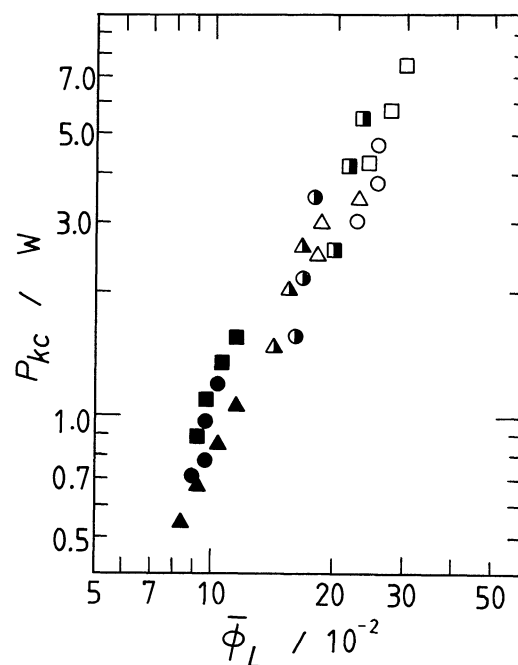


Fig. 10. Relation between $\bar{\phi}_L$ and P_{kc} at $V = 5.5 \times 10^{-3} \text{ m}^3$, SN: \circ ; (1.0×10^{-2} vol%) Detergent solution, \square ; (1.0×10^{-2} wt%) Saponin solution, Δ ; (5.0×10^{-2} wt%) Tween 40 solution. FIDA: \bullet ; (1.0×10^{-2} vol%) Detergent solution, \boxplus ; (1.0×10^{-2} wt%) Saponin solution, \blacktriangle ; (5.0×10^{-2} wt%) Tween 40 solution. MFRD: \bullet ; (1.0×10^{-2} vol%) Detergent solution, \blacksquare ; (1.0×10^{-2} wt%) Saponin solution, \blacktriangle ; (5.0×10^{-2} wt%) Tween 40 solution.

foam-ascending section when foam-breaking was carried out with SN¹³ or FIDA¹³) was evaluated in the same manner as in MFRD. The required power, P_{kc} , of SN and FIDA was calculated in terms of both the nozzle pressure, P_n , and the corresponding critical liquid feed rate, W_c . Figure 10 shows a typical plot of P_{kc} vs. $\bar{\phi}_L$. The data in the system with MFRD are also shown for a comparison. Foam-breaking systems with SN and FIDA as well have a tendency that P_{kc} becomes larger as $\bar{\phi}_L$ increases. This result shows that $\bar{\phi}_L$ can also be used as a measure to reflect a dynamic foaming capacity in a gas-bubbling system under foam-breaking with this configuration of foam-breaker.

Moreover, as can be seen in Fig. 10, the P_{kc} values at the critical foam-breaking state tend to be the lowest in the system with MFRD and the highest in the system with SN. The amount of liquid required for foam-breaking at the same U_g and V is smallest in MFRD and largest in SN. The higher values of P_{kc} in a system with SN are attributed to an increase of $\bar{\phi}_L$ in the foam layer caused by the splashing of large amounts of the liquids.

The authors wish to express their thanks to Professor Michihiro Fujii of the University of Niigata

for his kind suggestions about the preparation of this article.

Nomenclature

d_B	Foam size, m
D_d	Rotating disk diameter, m
D_f	Diameter of fixed disk underneath rotating disk ($=D_d$), m
D_T	Vessel diameter, m
h_f	Foam-ascending distance from aerated liquid surface, m
H_d	Disk height, m
H_f	Distance between H_d and H_L ($=H_d-H_L$), m
H_L	Static liquid height in vessel, m
N_c	Critical disk speed required for foam-breaking, s^{-1}
P_n	Nozzle pressure in SN and FIDA, Pa
P_{kc}	Power for foam-breaking, W
R	Distance from vessel wall, m
U_g	Gas velocity on cross-sectional area of vessel, $m\ s^{-1}$
V	Operating liquid volume in vessel, m^3
V_F	Foam volume, m^3
V_L	Net liquid volume in V_f , m^3
V_s	Equilibrium volume of foam above liquid layer, m
V_{tg}	Volumetric gas flow rate, $m^2\ s^{-1}$
W	Liquid feed rate onto rotating disk, $m^3\ s^{-1}$
W_c	Critical liquid feed rate in SN and FIDA, $m^3\ s^{-1}$
μ	Viscosity of liquid, Pas
ν	Kinematic viscosity of liquid, $m^2\ s^{-1}$
π	Ratio of circumference to diameter
ρ	Density of liquid, $kg\ m^{-3}$
σ	Surface tension of liquid, $N\ m^{-1}$
τ	Rotational torque of disk under foam-breaking, N m
ϕ_L	Local foam ratio
$\bar{\phi}_L$	Averaged foam ratio
Σ	Foaminess, s

References

- 1) M. Ito and A. Abe, "Kihō-Ekiteki Kōgaku," ed by Soc. Chem. Engrs. Jpn., Nikkankōgyō Shinbunsha, Tokyo (1969), Chap. 9.
- 2) J. J. Bikerman, "Foams," Springer-Verlag, New York (1973), Chap. 12.
- 3) M. J. Hall, S. D. Dickinson, R. Pritcard, and J. I. Evans, "Progress in Industrial Microbiology," ed by D. J. D. Hockenhull, Churchill Livingstone, London (1973), Vol. 12, pp. 170—234.
- 4) U. E. Viesturs, M. Z. Kristasovs, and E. S. Levitans, "Advances in Biochemical Engineering," Springer-Verlag, New York (1982), Vol. 21, pp. 169—224.
- 5) N. P. Ghildyal, B. K. Lonsane, and N. G. Karanth, "Advances in Applied Microbiology," Academic Press, New York (1988), Vol. 33, pp. 173—222.
- 6) T. Sasaki, "Hyōmenkōgaku Koza, 3. Kaimengenshō No Kiso," ed by T. Sasaki, Y. Tamai, T. Hisamatsu, and M. Maeda, Asakura Shoten, Tokyo (1973), pp. 155—202.
- 7) Y. Takahara, *Kagaku Sōchi*, **20**, 35 (1978).
- 8) Y. Takahara, *Hakkō to Kōgyō*, **36**, 288 (1978).
- 9) T. Sasaki, *Kōgyokagaku Zasshi*, **58**, 809 (1955).
- 10) A. Ohkawa, M. Sakagami, N. Sakai, N. Futai, and Y. Takahara, *J. Ferment. Technol.*, **56**, 428 (1978).
- 11) A. Ohkawa, N. Sakai, H. Imai, and K. Endoh, *Biotechnol. Bioeng.*, **26**, 702 (1984).
- 12) A. Ohkawa, Y. Ueda, and N. Sakai, *Chem. Lett.*, **1985**, 99.
- 13) Y. Sonoda, J. Someya, N. Futai, N. Tagaya, and T. Murakami, *Hakkōkōgaku Kaishi*, **51**, 479 (1973).
- 14) N. Futai, T. Murakami, and Y. Takahara, *Hakkōkōgaku Kaishi*, **54**, 808 (1976).
- 15) J. J. Bikerman, "Foams," Springer-Verlag, New York (1973), Chap. 6.
- 16) J. Biswass and R. Kummar, *Chem. Eng. Sci.*, **36**, 1547 (1981).
- 17) J. J. Bikerman, *Trans. Faraday Soc.*, **34**, 634 (1938).
- 18) S. Noguchi, *Kagaku To Seibutsu*, **10**, 39 (1972).
- 19) P. A. Hass and H. F. Johnson, *AIChE J.*, **11**, 319 (1965).
- 20) E. Rubin, C. R. LaMantia, and E. L. Gaden, Jr., *Chem. Eng. Sci.*, **22**, 1117 (1967).
- 21) K. K. Kalischewski, W. Bumblis, and K. Schügerl, *Eur. J. Appl. Microbiol. Biotechnol.*, **7**, 21 (1979).
- 22) M. Shiraishi, S. Horio, and K. Toyoshima, *Nippon Kagaku Kaishi*, **1983**, 724.